NEW DIGITAL SIMULATION TECHNIQUE FOR A CURRENT-SOURCE INVERTER FED SYNCHRONOUS MOTOR PART I

M.Y. Abdelfattah , M.M. Ahmed
Department of Electrical Engineering
Faculty of Engineering
Alexandria University
Alexandria, Egypt

ABSTRACT

The naturally-commutated current-fed synchronous motor has attained a greater part in the various industrial applications as a variable speed drive because of its simplicity and improved dynamic behaviour. The commutation in the inverter bridge is achieved by using the induced back e.m.f. of the armature windings and therefore no forced commutation devices are required which leads to lower costs. In this paper a novel accurate digital simulation technique is presented for the system. This technique is capable of predicting both transient and steady-state performance for a salient pole synchronous motor fed from a naturally-commutated current-source inverter. The effect of presence of damper windings on machine performance is investigated.

NOTATIONS

A,B,C	Suffices inducating stator variables as in i_A
q,d	Suffices indicating direct-and quadrature-axis respectively
0	Suffix indicating star point of stator armature as in V_{A0}
N	Suffix indicating inverter dc-link negative rail
R_F,L_F	Field winding resistance and self inductance respectively
R_D,L_D	Resistance and self inductance respectively for damper winding on d-axis
R_Q,L_Q	Resistance and self inductance respectively for damper winding on q-axis
R_a	Resistance of stator phase winding
L_d,L_q	Transformed inductances related to the actual three-phase machine stator windings
M_d	Transformed mutual inductance between a stator phase and the field winding and the d-axis damper winding
M_q	Transformed mutual inductance between a stator phase and the q-axis damper winding
M_{FD}	Mutual inductance between the field winding and the d-axis damper winding
θ	Angle between stator phase A and d-axis
ω_r	Rotational frequency of the machine rotor
J	Rotor moment of inertia
T_E	Electric torque developed
T_L	Mechanical Load torque
T_D	Drag torque
K	Friction constant
R_f,L_f	Filter resistance and inductance respectively
V_s	dc-source voltage
V_{dc}	Instantaneous dc-link voltage
γ	No-load angle of advance
p	Operator d/dt

INTRODUCTION

A synchronous motor fed from a naturally-commutated current-source inverter is very simple and has improved dynamic behaviour over other variable speed drives. The simplicity of this system over the more expensive and bulky forced-commutated thyristor inverter supplying a variable frequency ac machine is achieved when using natural commutation to commutate different thyristors in the inverter bridge. The machine armature windings induce voltages which commutate the machine currents through different conduction patterns. This can be done if the machine is over excited so that a leading power factor is present at its input terminals.

A considerable amount of work has been performed for the study of this system [1]-[7]. Most of these works have been concerned with the steady-state performance of the

system. All published papers, [1]-[7], put different asssumptions during the mathematical model calculations. These assum[tions such as constant link current, finite commutation period with linear variation, neglecting machine resistances, and/or constant field current may be accepted with certain conditions at steady-state but not during transient operation. In this paper a general equivalent circuit for the system shown in Figure (1) is developed. The inverter thyristors are triggered using a rotor position sensor which changes the firing pattern each 60° of the rotor angular position.

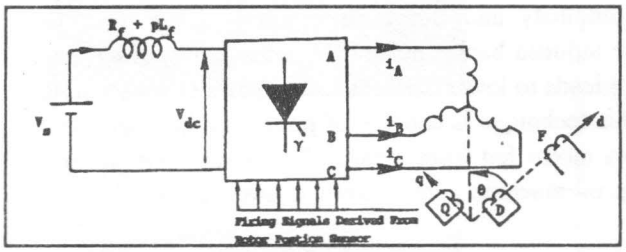

Figure 1. Schematic circuit for a current-source inverter fed synchronous motor.

GENERAL MODEL OF A SYNCHRONOUS MACHINE

The differential equations describing thee behaviour of a salient-pole synchronous machine with damper winding in the d-q frame of axes can be formulated from Figure (2) as follows:

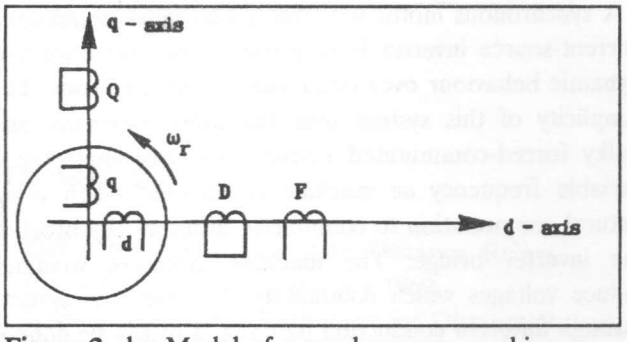

Figure 2. d-q Model of a synchrronous machine.

$$\mathbf{V} = [R]\,\mathbf{I} + [L]\,\mathbf{pI} \qquad (1)$$

where,

$$\mathbf{V} = [\,V_F \;\; V_d \;\; V_q \;\; V_D \;\; V_Q\,]$$

$$\mathbf{I} = [\,i_F \;\; i_d \;\; i_q \;\; i_D \;\; i_Q\,]$$

$$[L] = \begin{bmatrix} L_F & M_d & 0 & M_{FD} & 0 \\ M_d & L_d & 0 & M_d & 0 \\ 0 & 0 & L_q & 0 & M_q \\ M_{FD} & M_d & 0 & L_D & 0 \\ 0 & 0 & M_q & 0 & L_Q \end{bmatrix}$$

State Representation of a Synchronous Machine

Equation (1) can be rearranged in the following form:

$$\mathbf{pI} = -[L]^{-1}[R]\,\mathbf{I} + [L]]^{-1}\,\mathbf{V} \qquad (2)$$

where,

$$[L]^{-1} = \begin{bmatrix} AA1 & AA2 & 0 & AA3 & 0 \\ AA2 & AA4 & 0 & AA5 & 0 \\ 0 & 0 & AA6 & 0 & AA7 \\ AA3 & AA5 & 0 & AA8 & 0 \\ 0 & 0 & AA7 & 0 & AA9 \end{bmatrix}$$

The coefficients AA1 → AA9 are given n Appendix (I).

Torque Expression

The eelectric torque T_T can be expressed in per unit quantities by the following equation:

$$T_E = \mathbf{I}^t\,[G]\,\mathbf{I}$$

where,

$$[G] = \begin{bmatrix} 0 & 0 & 0 & 0 & 0 \\ 0 & 0 & L_q & 0 & M_q \\ -M_d & -L_d & 0 & -M_d & 0 \\ 0 & 0 & 0 & 0 & 0 \\ 0 & 0 & 0 & 0 & 0 \end{bmatrix}$$

The equation of motion is described by the following equation:

$$J\,P\omega_r + K\omega_r = T_E - T_L - T_D$$

Which can be rearranged as:

$$P\omega_r = [\, T_E - T_L - T_D - K\omega_r \,] / J$$

Transformation Between Different Reference Frames

Invarient transformation from three phase quantities (A,B,C) into d-q quantities can be represented by:

$$\begin{bmatrix} V_d \\ \\ V_q \end{bmatrix} = [C] \begin{bmatrix} V_{A0} \\ V_{B0} \\ \\ V_{C0} \end{bmatrix} \quad \&$$

$$\begin{bmatrix} i_d \\ \\ i_q \end{bmatrix} = [C] \begin{bmatrix} i_A \\ i_{B0} \\ \\ i_{C0} \end{bmatrix} \qquad (3)$$

Similar transformation from d-q into (A,B,C) can be represented by:

$$\begin{bmatrix} V_d \\ V_{B0} \\ \\ V_{C0} \end{bmatrix} = [C]^t \begin{bmatrix} V_d \\ \\ V_q \end{bmatrix} \quad \&$$

$$\begin{bmatrix} i_A \\ i_B \\ \\ i_C \end{bmatrix} = [C]^t \begin{bmatrix} i_A \\ i_{B0} \\ \\ i_q \end{bmatrix} \qquad (4)$$

$$[C] = \sqrt{\frac{2}{3}} \begin{bmatrix} \cos\theta & \cos(\theta-120^\circ) & \cos(\theta+120^\circ) \\ \\ \sin\theta & \sin(\theta-120^\circ) & \sin(\theta+120^\circ) \end{bmatrix}$$

DIGITAL SIMULATION FOR A cURRENTT-SOURCE INVERTER FED SYNCHRONOUS MACHINE

During the normal operation of a synchronous machine connected to a current source inverter, Figure (3), either two phases (conduction mode) or three phases (commutation mode) are connected to the dc supply. Table (1) shows all possible modes of normal operation.

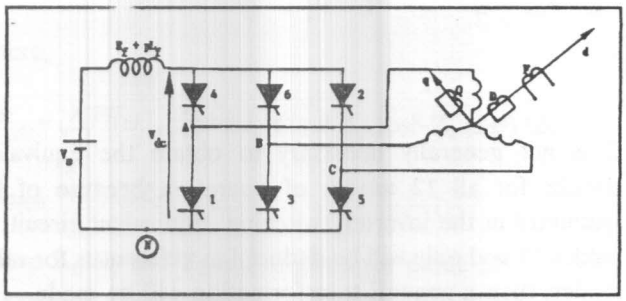

Figure 3. Current-source inverter fed synchronous machine.

Table 1. Possible Modes of Normal Operation

Mode	Thyristors Conducting	Mode	Thyristors Conducting
1	6,1	7	3,4
2	6,1,2	8	3,4,5
3	1,2	9	4,5
4	1,2,3	10	4,5,6
5	2,3	11	5,6
6	2,3,4	12	5,6,1

From Figure (3), it can be seen that:

$$\begin{aligned} V_{A0} &= V_{AN} + V_{NO} \\ V_{B0} &= V_{BN} + V_{NO} \\ V_{CO} &= V_{CN} + V_{NO} \end{aligned} \qquad (5)$$

By addition, keeping in mind that: $V_{A0}+V_{B0}+V_{CO}=0$, we get:

$$V_{NO} = -\,[V_{AN} + V_{BN} + V_{CN}\,] / 3 \qquad (6))$$

Substituting equations (5) and (6) into equation (3) we get :

$$\begin{bmatrix} V_d \\ \\ V_q \end{bmatrix} = [C] \begin{bmatrix} V_{AN} \\ V_{BN} \\ \\ V_{CN} \end{bmatrix} \quad (7)$$

$$\begin{bmatrix} V_{AN} \\ V_{BN} \\ \\ V_{CN} \end{bmatrix} = [C]^t \begin{bmatrix} V_d \\ \\ V_q \end{bmatrix} \quad (8)$$

It is not generally necessary to obtain the equivalent circuits for all 12 modes of operation because of the symmetry in the inverter switching. Equivalent circuit for modes 11 and only will be deduced as references for other modes, then a general transformation will be made.

Model 11

Figure (4) represents the connection when thyristors 5 and 6 are conducting, from this figure the following relations can be concluded:

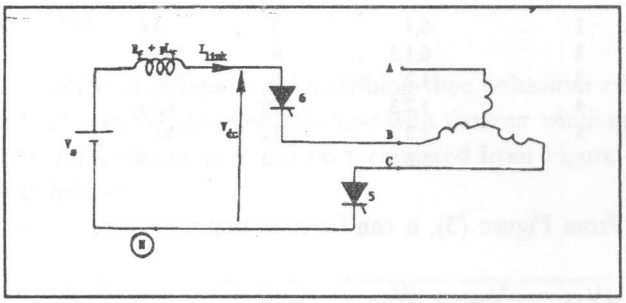

Figure 4. Circuit connection during mode 11.

$$V_{BN} = V_{dc}$$

$$V_{CN} = 0$$

From equation (8) we get :

$$V_{BN} - V_{CN} = \sqrt{2}\,[V_d \sin\theta - V_q \cos\theta]$$

i.e.

$$V_{dc} = \sqrt{2}\,[V_d \sin\theta - V_q \cos\theta] \quad (9)$$

Since phase A is opened:

$$i_A = 0 \quad \& \quad Pi_A = 0$$

$$i_B = I_{link}$$

$$i_c = - I_{link}$$

Substituting in equations (3) and (1), V_d and V_q can be deduced, then substituting in equation (9) we get:

$$V_{dc} = E_{(11)} + L_{M(11)}\, pI_{link} \quad (10)$$

Which can be represented by the equivalent circuit shown in Figure (5).

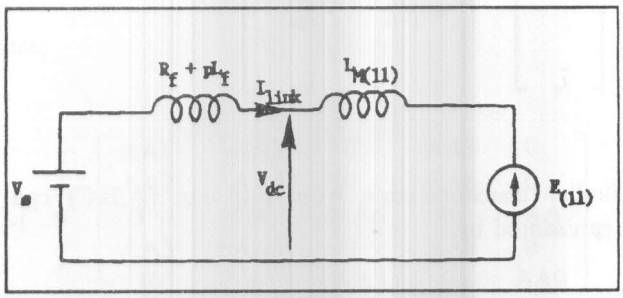

Figure 5. Equivalent circuit for mode 11.

where,

$$E_{(11)} = \sqrt{2}\,[Z_2 Z_3 \cos\theta - Z_1 Z_3 \sin\theta - Z_4 \sin\theta \cos\theta \{(i_d\omega_r - Z_2)\sin\theta - (i_q\omega_r + Z_1)\cos\theta\}]/Z_3$$

$$L_{M(11)} = 2Z_3/Z_5$$

$$Z_1 = [M_d (M_{FD} - L_D)(V_F - R_F i_F) - (L_D L_F - M^2_{FD})(R_a i_d + L_q \omega i_q + M_q i_Q \omega_r) - M_d (M_{FD} - L_F) R_D i_D]/D_1$$

$$Z_2 = [L_Q (M_d \omega_r i_F + L_d i_d \omega_r - R_a i_a i_q + M_d i_D \omega_r)/D_2] + [M_q R_Q i_Q / D_2]$$

$$Z_3 = [(L_D L_F - M^2_{FD})\cos^2\theta / D_1] + [L_Q \sin^2\theta / D_2]$$

$$Z_4 = [(L_D L_F - M^2_{FD})/D_1] - [L_Q/D_2]$$

$$Z_5 = [L_Q (L_D L_F - M^2_{FD})]/[D_1 D_2]$$

$$D_1 = L_F L_D L_D - M^2_d (L_F + L_D) - M^2_{FD} L_d + 2M_{FD} M^2_d$$

$D_2 = L_q L_q - M^2_q$

Mode 8

Figure (6) represents the connection when thyristors 3, 4 and 5 are

$V_{AN} = V_{dc}$

$V_{BN} = V_{CN} = 0$

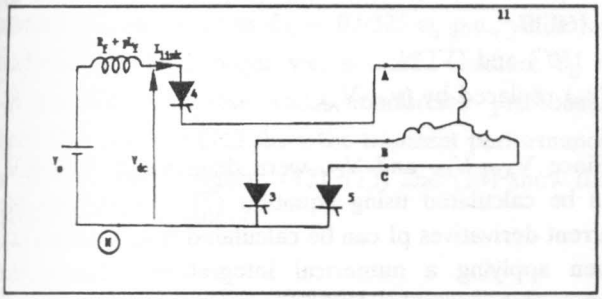

Figure 6. Circuit connection during mode 8.

Substituting in equation (8) we get:

$$V_d = \sqrt{2/3}\, V_{dc} \cos\theta$$
$$V_q = \sqrt{2/3}\, V_{dc} \sin\theta \qquad (11)$$

From Figure (6) and equation (4), it can be seen that:

$$I_{link} = i_A = \sqrt{2/3}\ [i_d \cos\theta + i_q \sin\theta]$$

Differentiating both sides give:

$$PI_{link} = \sqrt{2/3}\ [\cos\theta\ ppi_d - i_d \omega_r \sin\theta + \sin\theta\ pi_q i_q \omega r \cos\theta] \qquad (12)$$

Substituting equations (2) and (11) into equation (12) gives:

$$V_{ds} = E_{(8)} + L_{M(8)}\, pI_{link} \qquad (13)$$

Which can be represented by the equivalent circuit shown in Figure (7).

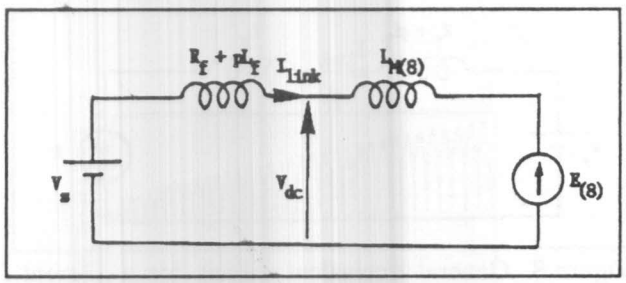

Figure 7. Equivalent circuit for mode 8.

where,

$$E_{(8)} = \sqrt{3/2}(\omega_r i_d \sin\theta - \omega_r i_q \cos\theta - Z_1 \cos\theta - Z_2 \sin\theta)/Z_3$$

$$L_{M(8)} = 3/(2Z_3)$$

where Z_1, Z_2 and Z_3 are as given for mode 11.

Symmetry Relations

Similar modes are related by the following linear transformation:

$$\begin{bmatrix} i_q^* \\ i_d^* \end{bmatrix} = \begin{bmatrix} \cos\lambda & -\sin\lambda \\ \sin\lambda & \cos\lambda \end{bmatrix} \begin{bmatrix} i_q \\ i_d \end{bmatrix}$$

Where the * indicates a transformed quantity, and

$\lambda = 0^\circ$ for modes 2, 5, 8 and 11

$\lambda = 120^\circ$ for modes 3, 6, 9 and 12

$\lambda = -120^\circ$ for modes 1, 4, 7 and 10

To generalize the equivalent circcuits obtained for modes 8 and 11, the angle θ is replaced by $(\theta - \lambda)$. Figure (8) represents the general equivalent circuit for a current-source inverter fed synchronous machine. Table (2) gives the values of E and L_M for the different operating modes.

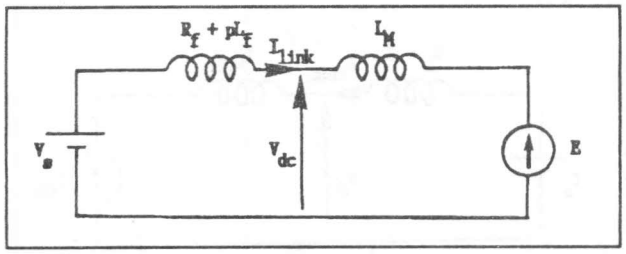

Figure 8. General equivalent circuit for a current-source inverter fed synchronous machine.

Table 2. Equivalent circuit parameters for different normal operating modes

Modes	L_M	E
2,4,6,8,10,12	$3/[2Z_3]$	$\sqrt{3/2}[\omega_r i_d \sin(\theta-\lambda)$ $-\omega_r i_q \cos(\theta-\lambda)-Z_1 \cos(\theta-\lambda)$ $-Z_2 \sin(\theta-\lambda)]/Z_3$
		$\sqrt{2[Z_2 Z_3 \cos(\theta-\lambda)}$ $-Z_1 Z_3 \sin(\theta-\lambda)-Z_4 \sin(\theta-\lambda)$
1,3,5,7,9,11	$2\ Z_3/Z_5$	$\cos(\theta-\lambda)\{(i_d\omega_r-Z_2) \sin(\theta-\lambda)$ $-(i_q\omega_r+Z_1) \cos(\theta-\lambda)\}]/Z_5$

From this known equivalent circuit V_{dc} can be calculated as follows:

$$pI_{link} = [(V_s-E)-R_f I_{link}]/[L_f+L_M]$$

$$V_{dc} = E + pI_{link} L_M$$

knowing V_{dc}, the phase voltages V_{AN}, V_{BN} and V_{CN} can be calculated according to the known conducting pattern. For example $V_{AN} = 0$ if thyristor 1 is conducting, $V_{AN} = V_{dc}$ if thyrisstor 4 is conducting and $V_{AN} = V_{ANOC}$ if both thyristors 1 and 4 are not conducting. V_{ANOC} is the open circuit emf of phase A and can be calculated from the following equation:

$$V_{ANOC} = \sqrt{3/2}\,[V_d \cos\theta + V_q \sin\theta] + [V_{dc}/2] \quad (14)$$

where,

$$V_q = [(i_d\omega_r-Z_2)\sin^2\theta-(i_q\omega_r+Z_1)\sin\theta\cos\theta+[L_D L_F - M^2_{FD})(V_{CN}-V_{BN})\cos\theta/(\sqrt{2}\,D_1)\}]/Z_3 \quad (15)$$

$$V_d = D_1[(i_d\omega_r-Z_2)\sin\theta-(i_q\omega_r+Z_1)\cos\theta-[L_Q \sin\theta V_q/D_2)]/[(L_D L_F-M^2_{FD})\cos\theta] \quad (16)$$

Similarly V_{BN} and V_{CN} can be calculated considering the following modifications:

1. If phase B is opened, V_{NOC} will be calculated using equations (14), (15) and (16) with θ replaced by (θ-120°) amd (V_{CN}-V_{BN}) replaced by (V_{AN}-V_{CN}).
2. If phase C is opened, V_{CNOC} will be calculated using equations (14), (15) and (16) with θ replaced by (68,17 + 120°) and (VCN -V_{BN}) replaced by (v_{BN}-V_{AN}).

Since V_{AN}, V_{BN} and V_{CN} were determined, V_d and V_q can be calculated using equation (7). Consequently the current derivatives pI can be calculated from equation (2). Then applying a numerical integration technique the system state variables (machine currents and speed) can be calculated.

NUMERICAL RESULTS

Using the simulation technique described in thee preceeding sections, steady state and dynamic performance for the system are carried out. The machine used for the prediction has the parameters and ratings given in Appendix (II).

A well known problem that is associated with operation of this system is the reduced commutation capability of the machine at very low speed includding starting from stand-still. Different methods are used to overcome this problem [8]-[11]. However, this is not the scope of this paper. For the purpose of the digital simulation the machine is assumed to be running at no-load with a speed of 0.5 p.u. with its field winding connected to the excitation source before being connected to the inverter so that the machine achieved its commutation ability.

Two different schemes are used for triggering the inverter thryristors. The first uses a rotor position sensor [8]-[9]. The second senses the zero crossing of the armature line-to-line voltage [10]-[11]. The first scheme is adopted for the digital silulation. This technique provides the firing pulses according to the no-load zero-voltage crossing. This firing angle is called the no-load angle of advance γ. In this scheme the firing patterns changes

every 60° of te rotor angular position. The firing angle γ was chosen to be 80° for the digital simulation prediction. During the simulation process, Euler method of numerical integration was used. The time increment Δt was chosen to be 0.01 p.u. for the computer program executions.

Steady-state and dynamic performances are carried out for the following three different cases:

1. Salient-pole machine with damper windings.
2. Salient-pole machine without dampper windings.
3. Nonsalient-pole machine without damper windings.

For transient performance prediction, the load torque is assumed to have the form $T_L = 0.9325\ \omega_r$ p.u., while for steady-state the load torque was assumed constant T_L = 0.28 p.u. for the three cases mentioned previously. Figures (9), (10) and (11) show the transient performance for the three cases. Figures (12), (13) and (14) show the steady-state performances.

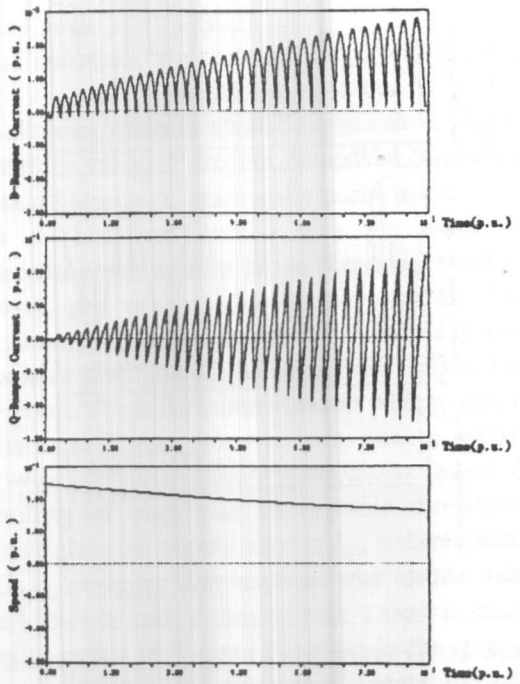

Figure 10. Transient performance continued.

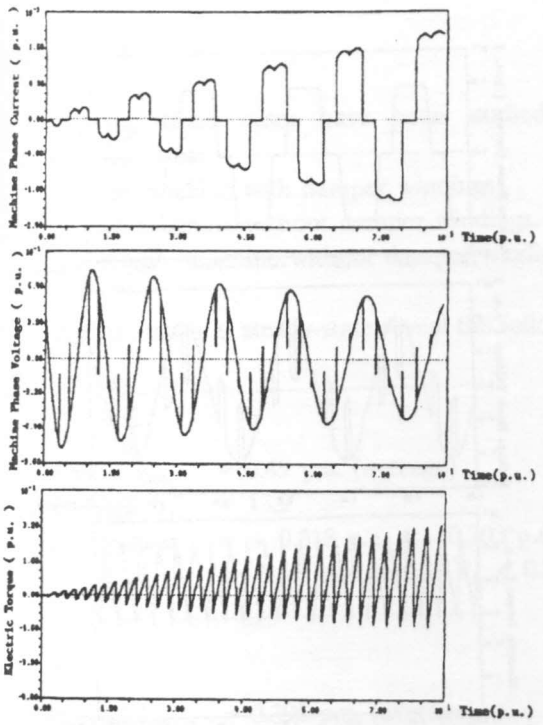

Figure 9. Transient performance for salient-pole synchronous motor with damper windings.

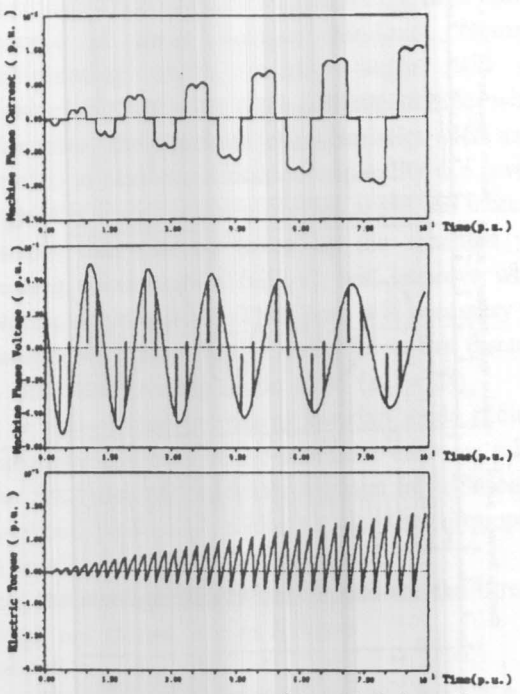

Figure 10. Transient performance for salient-pole synchronous motors without damper windings.

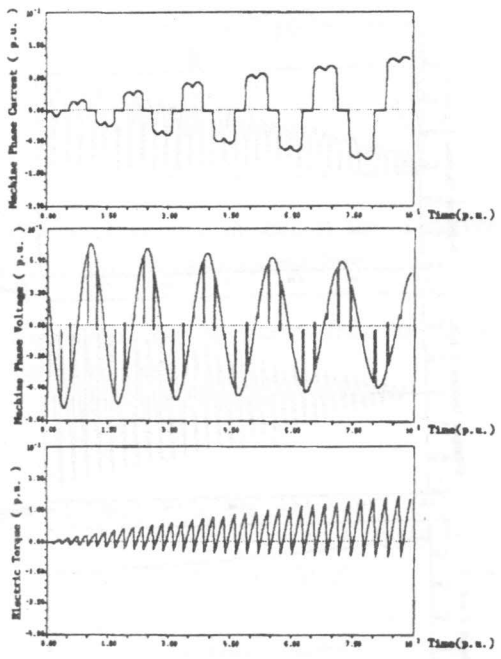

Figure 11. Transient performance for nonsalient-pole synchronous motor without damper windings.

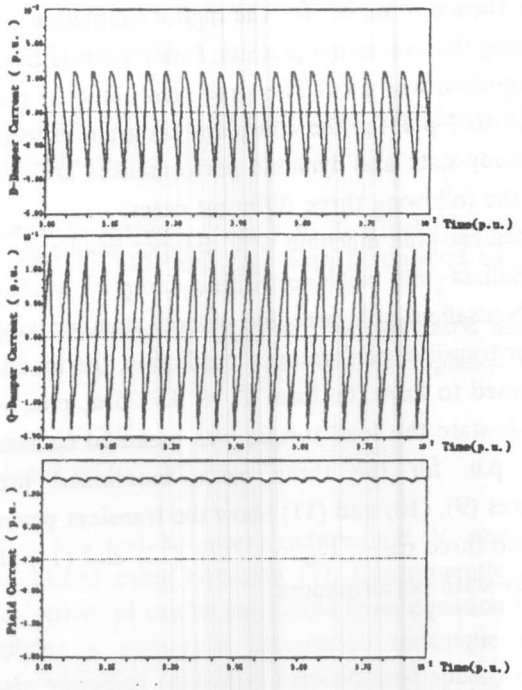

Figure 12(b). Steady-state performance continued.

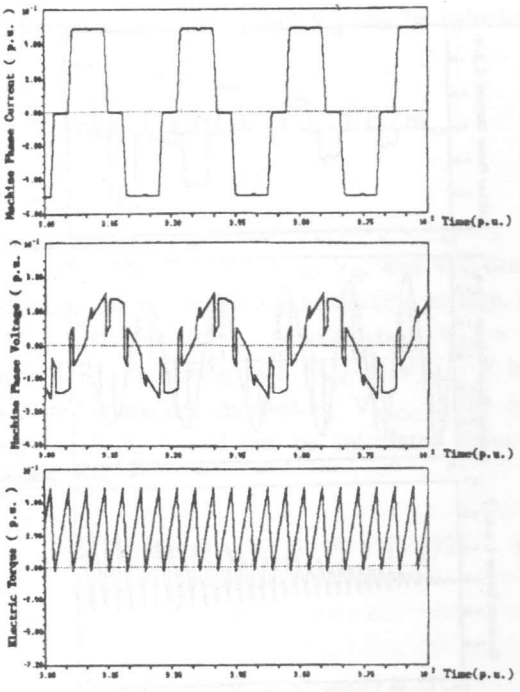

Figure 12, Steady-state performance for salient-oile synchronous motor with damper windings.

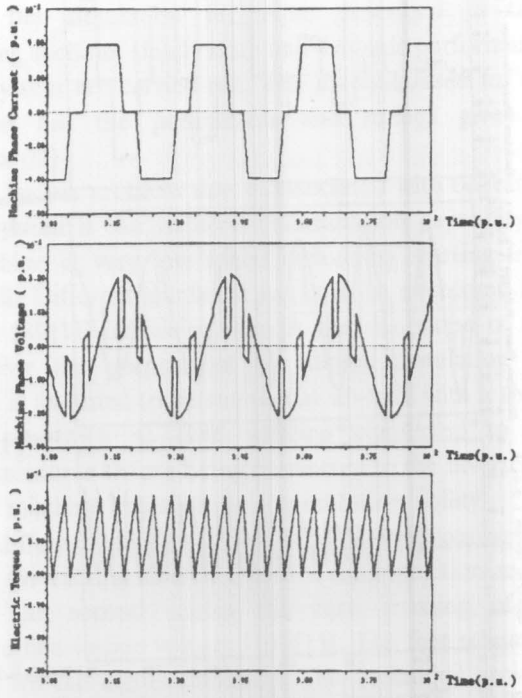

Figure 13. Steady-state peerformance for salient-pole synchronous motor without damper windings.

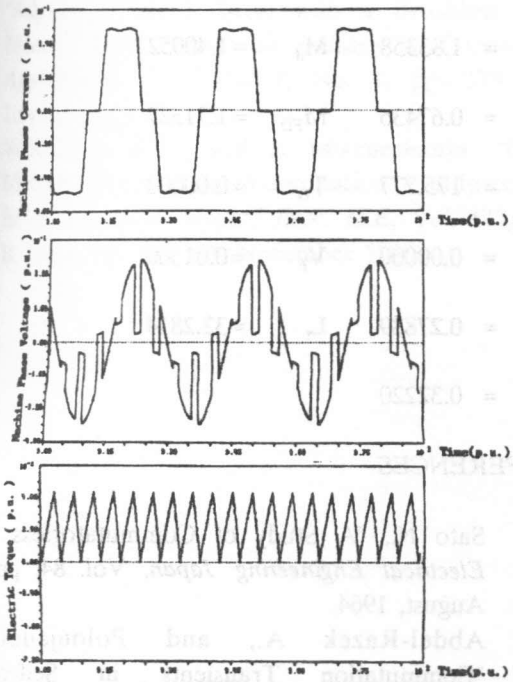

Figure 14. Steady-stae performance for nonsalient-pole synchronous motor without damper windings.

CONCLUSION

The following three cases have been studied foor comparison purposes:

1. Salient-pole machine with damper windings.
2. Salient-pole machine without damper windings.
3. Nonsalient-pole machine without damper windings.

The computed results at steady-state reveal the following:

Case 1

Link current $I_{link(1)}$ = 0.49 p.u. (average)
Overlap angle μ_1 = 13.9°
Torque pulsation = + 0.318 p.u. & - 0.303 p.u. from average load torque T_L = 0.28 p.u.

Case 2

Link current $I_{link(2)}$ = 0.396 p.u. (average)
Overlap angle μ_2 = 20.3°
Toorque pulsation = + 0.292 p.u. & - 0.303 p.u. from average load torque T_L = 0.28 p.u.

Case 3

Link current $I_{link(3)}$ = 0.29 p.u. (average)
Overlap angle μ_3 = 20.3°
Torque pulsation = + 0.251 p.u. & -0.268 p.u. frrom average load torque T_L = 0.28 p.u.

The following remarks should explain these figures:

1. Armature currents are not sinusoidal, therefore they contain harmonics. Harmonics occur in pairs (i.e. 5th, 7tth & 11th etc.) which give the same velocity differences with respect to synchronous speed and, as a result, give rise to induced rotor currents of similar frequency. Hence, currents will be induced in any rotor circuit to give an induction machine action for each harmonic. These harmonic currents will produce torque pulsations. These pulsation are due to phase shift between different harmonic which is caused due to travelling of each pair in opposite directions. The figures given for supply current I_{link} indicate that: $I_{link(1)} > I_{link(2)} > I_{ink(3)}$. This explains why torque pulsations are higher in case 1 than in case 2 than in case 3.
2. The presence of damper windings in the rotor causes a considerable reduction of armature reaction reactance over the leakage reactance. Therefore the commutating reactance offered by the machine will be much less when damper windings exist than that in the absence of these damper windings. Hence, the commutating angle, overlap angle, will reduce considerably when the rotor contains damper windings. Moreover, the machine characteristics such as speed regulation and commutation capability (i.e. over load capability since reducing overlap angle will increase the current that can be taken by the machine without causing commutation failure), will improve when the overlap angle is small. Therefore it is necessary to have damper wwindings in the rotor. From this discussion it is clear that overlap angle $\mu_1 < (\mu_2 = \mu_3)$.
3. It is known that increasing overlap angle reduces the harmonic contents of the armature currents relative to the fundamental, and this explain in addition to the previous explination given in 1 why the torquepulsation is smaller in case 3 than in case 1.

Also, the average steady-state speed for the three cases, although not shown, are as follows:

$\omega_{r(1)} = 0.246$ p.u. $\omega_{r(2)} = 0.251$ p.u. $\omega_{r(3)} = 0.225$ p.u.

From these figures it is clear that the effect of damper

windings on the steady-state speed is small for the same load torque. Moreover, for non-salient pole machine the steady-state speed is lower than when saliency is present. Furthermore, field current, electric torque, damper currents, link current, and speed all have sixth harmonic components. Also, the field current fluctation is found to be slightly smaller for salient-pole machine with damper windings.

APPENDIX (I)

$D_1 = L_F L_d L_D - M^2_d(L_F + L_D) - M^2_{FD} L_d + 2M_{FD} M^2_d$

$D_2 = L_q L_Q - M^2_q$ $\quad AA1 = [L_d L_D - M^2_d]/D_1$

$AA2 = M_d[M_{FD} - L_D]/D_1$ $\quad AA3 = [M^2_d - L_d M_{FD}]/D_1$

$AA4 = [L_D L_F - M^2_{FD}]/D_1$ $\quad AA5 = M_d[M_{FD} - L_F]/D_1$

$AA6 = L_Q/D_2$ $\quad AA7 = -M_q/D_2$

$AA8 = [L_d L_F - M^2_d]/D_1$ $\quad AA9 = L_q/D_2$

APPENDIX (II)

The machine parameters used for simulation are taken from reference [7]. The machine ratings are 10hp, 220 V, 20 A, 60 Hz, 4-poles. The following base quantities are used:

$I_{base} = 20\sqrt{2}$ Amps. (Peak rated phase machine current)

$V_{base} = 220\sqrt{2/3}$ Volts (Peak rated phase machine voltage)

$f_{base} = 60$ Hz

Using these base quantities, the different parameters in per-unit are:

$R_a = 0.03933$ $\quad R_D = 0.07203$

$R_Q = 0.06556$ $\quad R_F = 0.01013$

$L_d = 1.77493$ $\quad L_q = 0.88450$

$L_D = 1.83910$ $\quad L_Q = 0.83107$

$L_F = 1.83358$ $\quad M_d = 1.40052$

$M_q = 0.67436$ $\quad M_{FD} = 1.71527$

$J = 175.777$ $\quad T_D = 0.00000$

$K = 0.00000$ $\quad V_F = 0.01500$

$R_f = 0.27889$ $\quad L_f = 32.2814$

$V_s = 0.32220$

REFERENCES

[1] Sato N., "A Study of Commutatorless Motor," *Electrical Engineering Japan*, Vol. 84, pp. 42-52, August, 1964.

[2] Abdel-Razek A., and Poloujadoff M., "Commutation Transients in Selfcontrolles Synchronous Machines Connected To D.C. Networks," *Electric Machines and Electromechanics*, Vol. 1/1, pp. 11-23, 1976.

[3] Williamson A.C., Issa N.A.H., and Makky A.R.A.M., "Variable-Speed Inverter-fed Synchronous motor employing natural commutation," *Proc. IEE*, Vol. 125, No.2, pp. 113-119, February 1978.

[4] Abdel-Razek A.A., and Poloujadoff M., "Analytical Approach To The Operation of A Synchronous Machine Associated With a Thyristor Bridge," *Electric Machines and Electromechanics, Vol. 3/2, pp. 167-184, 1978.*

[5] Frederick C., Brickhurst, "Performance Equations for DC Commutatorless Motoors Using Salien-pole Synchronous-Type Machines," *IEEE Trans. pn Industry Applications,* Vol. IA-16, No. 3, pp. 362-371, May/June 1980.

[6] Teruo Kataoka and Shoji Nishikata, "Transient Performance Analysis of Self-Controlled Synchronous Motors," *Ieee Trans. on Applications*, Vol. IA-17, No. 2, pp. 152-159, March/April, 1981.

[7] Chandrasekhar Namuduri and Paresh Sen C., "Digital Simulation of an Inverter-Fed Self-Controlled Synchronous Motor," *IEEE Trans. on Industrial Electronics,* Vol. IE-34, No. 2, pp. 205-215, May, 1987.

[8] Noriaki Sato and Vsevolod V. Semenov, "Adjustable Speed Drive with a Brushless DC Motor," *IEEE Trans. on Industry and General Applications,* Vol. IGA-7, No. 4, pp. 539-543, July/August 1971.

[9] Williamson A.C., and J. Mwenechanya, "New Method of Low-speed Commutation of an Inverter-fed Synchronous Motor," *Proc. IEE*, Vol. 127, Pt. B, No. 6, pp. 375-381, November 1980.

[10] Allan B. Plunkett and Fred G. Turnbull, "Load-Commutated Inverter/Synchronous Motor Drive Without a Shaft Position Sensor," *IEEE Trans. on Industry Applications*, Vol. IA-15, No. 1, pp. 63-71, Jan/Feb. 1979.

[11] Jacques Davoine, Robert Perret, and Hoang Le-Huy, "Operation of a self Controlled Synchronous Motor Without a Shaft Position Sensor," *IEEE Trans. on Industry Applications*, Vol. IA-19, No.2, pp. 217-222, March/April, 1983.